An Embedded Polygon Strategy for Quality Improvement of 2D Quadrilateral Meshes with Boundaries

Muhammad Naeem Akram, Lei Si and Guoning Chen[a]
University of Houston, Houston, U.S.A.

Keywords: Quadrilateral Meshes, Quality Improvement, Embedded Polygon.

Abstract: Quadrilateral (or quad) meshes generated by various remeshing and simplification methods for input models with complex structure and boundary configurations often possess elements with minimal quality, which calls for an optimization approach to improve their individual elements' quality while preserving the boundary features. Many existing methods either fix boundary vertices during optimization or assume a simple boundary configuration. In this paper, we introduce a new quality improvement framework for 2D quad meshes with open boundaries. Our framework aims to optimize the configuration of an embedded polygon constructed based on the one-ring neighbors of each interior vertex. A feature-preserved boundary optimization is also introduced based on the angle configuration of the individual boundary vertices to further improve the quality of the boundary elements. Our framework has been applied to a number of 2D quad meshes with various boundary configurations and compared with other representative methods to demonstrate its advantages.

1 INTRODUCTION

Quadrilateral (or quad) meshes are preferred by many mechanical engineering applications due to their desired properties for numerical simulations (Gao et al., 2017). Numerous efforts have been made to address the generation of high-quality quad meshes (Bommes et al., 2009; Bommes et al., 2013; Campen, 2017; Fang et al., 2018; Viertel and Osting, 2019; Docampo-Sanchez and Haimes, 2019). Nonetheless, robustly generating high-quality quad meshes for input with arbitrary geometry and topology remains a challenge. Most methods produce initial quad meshes with sub-optimal quality which require a post-processing to improve the element quality by re-positioning the vertices. This post-processing is called mesh quality improvement. If done properly, mesh quality improvement can significantly improve the quality of a mesh (see Figure 5).

Existing quad mesh quality improvement techniques either apply a local tangential space smoothing (Sorkine, 2005; Daniels et al., 2009; Xu et al., 2018) after mesh generation or perform re-parameterization, re-sampling, or edge flipping (Ben-Chen et al., 2008; Tarini et al., 2011; Pietroni et al., 2009; Prasad, 2018; Gao et al., 2015) during mesh processing. The smoothing approach preserves the mesh connectivity which is required for structured mesh improvement. However, this constraint may limit its capability of improving meshes with challenging connectivity configurations. In contrast, the re-parameterization, re-sampling, or edge-flipping methods optimize the local mesh connectivity to achieve better element quality, while sacrificing the preservation of the structure of the mesh (i.e., introducing additional irregular vertices). In this work, we focus on the former approach.

Most times, the quality of a quad mesh can be measured by the scaled Jacobian measures (Pébay et al., 2007). By definition, the scaled Jacobian measure of each quad is determined by it's four interior angles. A perfect scaled Jacobian (i.e., 1) can be achieved if all four interior angles are $90°$. If one angle is larger than $180°$, the scaled Jacobian becomes negative, and the element with negative Jacobian is referred to as an *inverted element*. An effective quality improvement technique should remove inverted elements in the mesh as much as possible. For simple quad meshes with non complex structure and boundaries, smoothing methods like Laplacian mesh smoothing work well and generate high-quality elements, but for quad meshes with complex boundaries (e.g., with many small and sharp features), further optimization and element refinement is vital in tackling the inverted elements, preserving features, and smoothing the mesh.

This paper introduces a new quality improvement

[a] https://orcid.org/0000-0003-0581-6415

Akram, M., Si, L. and Chen, G.
An Embedded Polygon Strategy for Quality Improvement of 2D Quadrilateral Meshes with Boundaries.
DOI: 10.5220/0010209101770184
In *Proceedings of the 16th International Joint Conference on Computer Vision, Imaging and Computer Graphics Theory and Applications (VISIGRAPP 2021) - Volume 1: GRAPP*, pages 177-184
ISBN: 978-989-758-488-6

technique, aiming to improve the Jacobian measures of the mesh. Our method is inspired by Xu and Newman's approach (Xu and Newman, 2005) that optimizes the position of a vertex of each quad to be closer to the bi-sector line of its opposite corner. Different from their method, we optimize the configuration of an embedded polygon surrounding an interior vertex based on its direct one-ring neighbors (see Figure 1). Furthermore, a boundary optimization strategy is introduced to optimize the positions of boundary vertices based on their angle configuration, while still preserving boundary features. This enables further improvement of the quality of the quad elements at the boundary. We have applied our method to a number of quad meshes produced by some quad mesh generation and simplification processes. We compared the quality of the optimized meshes obtained using our method with those obtained with Xu and Newman's method (Xu and Newman, 2005), Laplacian smoothing (Sorkine, 2005), and Mesquite (Brewer et al., 2003). The comparison shows that the optimized meshes with our method usually have higher minimum and average scaled Jacobians than those produced by other methods.

2 RELATED WORK

Two different groups of methods have been proposed for mesh quality improvement, i.e., smoothing and optimization with fixed mesh connectivity (Vartziotis and Himpel, 2014; Xu et al., 2018) and local connectivity modification (Prasad, 2018; Tarini et al., 2010; Gao et al., 2017). The present work belongs to the former group; thus, we review some representative methods in this group.

Among all smoothing techniques, Laplacian smoothing is the most popular technique that aims to move the individual interior vertices of a mesh toward the average of their direct neighbors. A recent work shows that Laplacian smoothing is essentially optimizing the mean ratio quality measure (Vartziotis and Himpel, 2014). Both explicit (iterative) method and implicit (direct solving) method (Ji et al., 2005) of Laplacian smoothing have been proposed. Interested readers should refer to (Sorkine, 2005; Vartziotis and Himpel, 2014) for a thorough review of Laplacian smoothing and its many variations. Despite its simplicity and popularity, Laplacian smoothing often fails for meshes that have undesired connectivity (especially near the concave area of the boundary) (Canann et al., 1998). Later, optimization-based, physics-based, or local (Kim et al., 2015) approaches were introduced to address the limitations of Laplacian smoothing with various levels of success.

Many quad mesh quality improvement methods are adapted from the techniques for triangle meshes (Canann et al., 1998), including Laplacian smoothing and its variations. Zhang et al. (Zhang et al., 2005) proposed a surface mesh smoothing technique by moving vertices along normal direction based on a surface diffusion flow. Xu and Newman (Xu and Newman, 2005) introduced an angle-based optimization to optimize the position of each vertex of a quad to be closer to the bi-sector line of its opposite corner and neighboring quads. An angle-based smoothing strategy was introduced by Zhou and Shimada (Zhou and Shimada, 2000) for 2D triangle meshes, which was later extended by Xu et al. (Xu et al., 2018) for the hexahedral mesh quality improvement. Most recently, machine learning technique has been applied to help address the untangling and smoothing of meshes (Kim et al., 2020). Our smoothing strategy is most similar to Xu and Newman's approach (Xu and Newman, 2005) but with an important difference, that is, we consider the bisectors of an embedded polygon of each interior vertex (see Figure 1), which reduces the number of angles for consideration by half. In addition, we include weighting strategy and boundary optimization to further improve the mesh quality.

3 OUR METHOD

We propose a smoothing method that makes use of circumjacent angles of a vertex to achieve regularization of an embedded polygon formed by one-ring neighbors. This approach is inspired by a former formulation of an energy function defined by a torsion springs system. Essentially, the energy based on a system of torsion spring for a vertex in a mesh can be defined as (Zhou and Shimada, 2000):

$$E = \sum_{i=0}^{2(n-1)} \frac{1}{2} K \theta_i^2 \tag{1}$$

where, n is the number of polygons incident to the vertex, θ_i is the angle between a side of the polygon and the edge connecting the vertex to the polygon, and K is a constant. It is not too difficult to see E is minimum when all θ_i are identical.

Consider a vertex with n neighbors directly connected to it as shown in Figure 1(a). In this example, vertex v has four neighbors: v_1, v_2, v_3 and v_4. A polygon can be constructed by connecting the neighboring vertices of v successively. We call such a polygon an embedded polygon of v as shown with dashed edges in the example of Figure 1 (a). The shape of

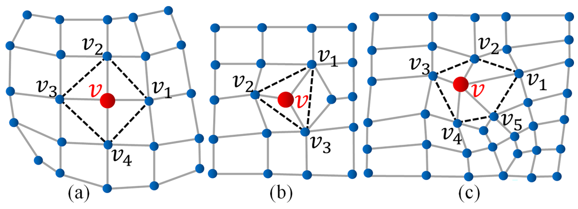

Figure 1: Examples embedded polygons for a valence-4 regular vertex (a), a valence-3 interior vertex (b), and a valence-5 vertex (c), respectively.

the embedded polygon depends on the number of the one-ring neighbors adjacent to source vertex (or the valence of the vertex) (Figure 1(a-c)). The circumjacent angles to a vertex are inherently the interior angles of the embedded polygon. A regular embedded polygon implies that all the interior angles are equal in magnitude and the source vertex is the centroid of the embedded polygon being equidistant from all the adjacent neighbors. In this ideal configuration, the angle bisectors of all the interior angles meet at a single point. For irregular polygons, however, the interior angles differ in magnitude and the angle bisectors of all the interior angles are not equivalent. Thus, the goal of optimizing the embedded polygon is to make it as regular as possible, so that the intersections of the individual bisectors converge to a point, which corresponds to the ideal position of the center vertex.

3.1 Embedded Polygon Optimization

Given a source vertex and its embedded polygon as illustrated in Figure 2, the position of the vertex can be updated based on angle bisectors of the interior angles. In an ideal regular polygon, the centroid bisects all the interior angles of the polygon and the following relation holds true:

$$\sum_{i=1}^{n}(x_i - X) = 0 \tag{2}$$

where, n is the number of one-ring neighbors of a vertex v or sides of the embedded polygon of v, x_i is the i_{th} angle bisector, and X is the centroid of the embedded polygon. For irregular polygons, solving the above equation yields:

$$X = \frac{1}{n}\sum_{i=1}^{n} x_i \tag{3}$$

Therefore, the optimal position of a source vertex v in its embedded irregular polygon can be achieved in the following two steps:

1. By updating the interior angles of the embedded polygon to be identical thus minimizing the energy function given by Eq.(1).
2. By updating the position of the source vertex to its optimal value as evidenced by Eq. (3).

In (Xu and Newman, 2005), angles formed by all the edges between successive neighboring vertices (adjacent and non-adjacent) are considered while updating the position of the source vertex.

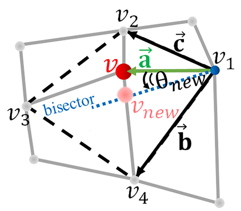

Figure 2: Vertex rotation to bisect interior angle of the embedded polygon.

In contrast, our approach considers the interior angles of the embedded polygon. Therefore, the number of angles under consideration is reduced in half. From Figure 2, the interior angles can be bisected by rotating the vectors formed by an edge between source vertex and the corners of the embedded polygon. For an interior angle θ, the extent of rotation for the vector $\mathbf{a}$ to bisect the interior angle can be found as:

$$\theta_{new} = \frac{1}{2}\left(\cos^{-1}\left(\frac{\mathbf{a}\cdot\mathbf{b}}{\|\mathbf{a}\|\|\mathbf{b}\|}\right) - \cos^{-1}\left(\frac{\mathbf{a}\cdot\mathbf{c}}{\|\mathbf{a}\|\|\mathbf{c}\|}\right)\right) \tag{4}$$

$$\mathbf{a}_{new} = \mathbf{b} + R\mathbf{a} \tag{5}$$

$$\text{where, } R = \begin{bmatrix} \cos\theta_{new} & -\sin\theta_{new} \\ \sin\theta_{new} & \cos\theta_{new} \end{bmatrix}$$

3.2 Interior Vertex Optimization

The rotation of the vertex v to bisect the n interior angles of the embedded polygon produces a set of n new coordinates. Consider a set $A = \{a_1, a_2, a_3, a_4\}$ of new coordinates for vertex v generated by its rotation set $B = \{\theta_1, \theta_2, \theta_3, \theta_4\}$ to bisect the interior angles of the embedded polygon. Each of the new coordinates is a candidate for moving the source vertex towards the optimal position. The final position of the source vertex can be calculated by:

$$v_{new} = \frac{1}{n}\sum_{i=1}^{n} a_i \tag{6}$$

This process is analogous to finding an optimal position of the source vertex through Laplacian smoothing. However, assigning equal weights to all of the candidate coordinates can have undesirable effects during smoothing and the process can sometimes get stuck between local minimums. To avoid such situations, weights can be assigned to each item of the candidate coordinates set A such that the movement of the source vertex is closest to the optimal position. For a candidate a in the coordinate set A generated by its corresponding θ in B, the weight can be assigned according to the following criteria:

$$w = 1 - \frac{|\theta|}{\sum_{i=1}^{n} |\theta_i|} \tag{7}$$

where, $\sum_{i=1}^{n} |\theta_i|$ represents the sum of all rotation angles for vertex v in B. The weights are assigned to each candidate such that rotation of vertex v for the worst interior angles bisection of the embedded polygon of v is favored. In this way, the regularity of the embedded polygon as well as approximation of the optimal position for vertex v is achieved at a faster speed since in later iterations of the smoothing process, the already bisected angle will have a smaller weight. The new coordinates v_{new} for the source vertex v can be calculated using weights as:

$$v_{new} = \lambda\left(\sum_{i=1}^{n} w_i a_i - v\right) \tag{8}$$

λ is a parameter to control the speed of optimization. For Laplacian smoothing different λ may affect the quality of the output. However, in our experiment, when varying λ between 0.1 and 1, no obvious impact is observed, but larger λ usually results in faster optimization process. Thus, we set $\lambda = 1$. The above method is similar to Laplacian smoothing (Sorkine, 2005) where the weights are used to determine the optimal position of a vertex. Hence, the regularity of the embedded polygon is achieved by making its interior angles close to the ideal angles through the first part of our approach (Section 3.1) while the optimal position of the source vertex v in its embedded polygon is achieved through the second part (Section 3.2) of our approach.

We incorporate collective energy minimization for the termination decision. The collective energy $E_{total} = \sum_i^n E_i$, where E_i is given by Eq.(1), can be computed by calculating and aggregating the energies of individual embedded polygons associated with each vertex being optimized. As the optimization advances, collective mesh energy is calculated before and after each optimization step and the optimization is terminated if $|E_{new} - E_{old}| < \tau$, where τ is a threshold used to determine termination decision.

3.3 Boundary Optimization

Feature preservation is usually required during mesh optimization where certain areas of the mesh are deemed important in terms of sharp features and corners and such areas must be preserved during the mesh optimization to keep the output mesh as close to the input mesh as possible. In our proposed approach, we extract the boundary of the input mesh and regard it as the reference for boundary optimization and feature preservation. The corners in the boundary are set as immobile (i.e., fixed during boundary optimization). A corner is a boundary vertex whose valence is not regular (i.e., the number of quads adjacent to this vertex is not 2). To preserve the portion of the boundary with large curvature and sharp features, we also mark boundary vertices whose two boundary edges form an angle θ_b such that $|\theta_b - 180°| > c$ (e.g., $c = 45°$ in our experiments). Most of the times, the sharp features are also singularities as in the case of Figure 3.

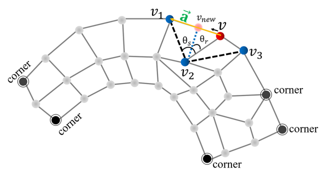

Figure 3: An example illustrating boundary optimization.

A boundary vertex with regular valence (or not marked as a corner) has a half embedded polygon with only one full interior angle as shown in Figure 3.

Since only one interior angle is optimized, the second part of our method is omitted for boundary optimization. The boundary vertices can be optimized in two ways:

- **Approach 1:** Similar to the interior vertices, boundary vertices can be rotated to bisect the interior angle of the embedded polygon. The boundary vertex in this case deviates from the boundary and remapping is required to snap the drifted vertex back to the original boundary. However, some of the input examples might have complex boundary configuration as shown in Figure 4 (middle) where the two regions of boundary are very close to each other and can lead to boundary vertex being snapped to wrong position.
- **Approach 2:** The boundary vertices can be restricted to move along the boundary only. From Figure 3, the new position of vertex v to bisect the interior angle of the embedded polygon can be calculated as follows:

$$v_{new} = v + \left(\frac{\theta_r}{\theta_s} \|a\|\right)\hat{a} \tag{9}$$

Although Approach 2 is more robust than Approach 1 in handling complicated boundary configurations, as evidenced by Figure 4, in our experiments, we have observed that the first approach sometimes produces meshes with better quality for meshes with

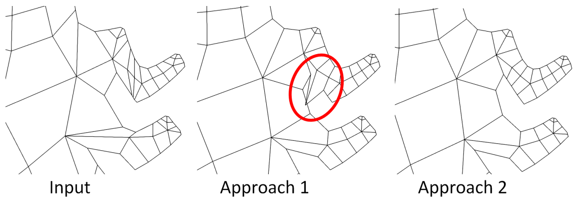

Figure 4: A boundary vertex is incorrectly mapped to a different part of the boundary after the boundary optimization using the first approach (middle). In contrast, the second approach preserves the boundary better (right).

simpler boundary configuration (e.g., no or little sharp features/corners). Therefore, the user can choose either of these two approaches to achieve a trade off between better quality and better boundary preservation. For both approaches, the boundary optimization is performed iteratively. We use a similar strategy for termination of boundary optimization as described in Section 3.2 with the same threshold τ. Our complete optimization framework incorporates the above boundary optimization and the interior vertex optimization.

4 RESULTS

We have applied the proposed quality improvement framework to a number of 2D quad meshes with varying boundary configurations and mesh connectivity. Table 1 provides the statistics of the meshes, their quality before and after optimization, and the run times. Figure 5 visualizes some representative meshes before and after optimization with our method. We use a saturation color coding to show the individual element quality measured by their scaled Jacobian. Red indicates low quality elements (i.e., small scaled Jacobian values) and white indicates elements with high scaled Jacobian values. From these results, we can see that the proposed optimization framework significantly improves the quality of all these meshes in terms of their minimum and average scaled Jacobian. The maximum scaled Jacobian of some meshes does drop slightly, as it gives more room for more elements to improve. In practice, the quality of the simulations (or other scientific computation) run on those meshes depends on the minimum and average scaled Jacobian measures as shown by Gao et al. (Gao et al., 2017).

Comparison with Xu and Newman's Approach. Figure 6 shows the comparison of our method with Xu and Newman's approach. Since their approach assumes fixed boundary vertices during optimization, to ensure a fair comparison we disable our boundary optimization for this comparison. Table 2 provides the quality statistics of the meshes produced with the two approaches. Our method without boundary optimization generates meshes with better minimum scaled Jacobian for almost all meshes. More importantly, our method without boundary optimization produces meshes with better average scaled Jacobian than Xu and Newman's method for all meshes.

Comparison with Laplacian Smoothing and Mesquite. Here, we compare with two different variants of Laplacian smoothing, i.e., the Laplacian with cotangent weights (which we will simply refer to as Laplacian), and a Laplacian smoothing implemented in a popular mesh quality improvement tool, Mesquite. Similar to the previous comparison, since both Laplacian smoothing methods assume fixed boundaries (otherwise, the mesh will shrink), we compare our method without boundary optimization with these two Laplacian smoothing. Figure 7 shows the meshes produced with the two Laplacian smoothing and our method without boundary optimization. Table 2 provides the quality statistics of the meshes produced with the two Laplacian smoothing methods, labeled as Laplacian and Mesquite, respectively. From this comparison, we see our method without boundary optimization outperforms the classic Laplacian (with cotangent weight) in almost all meshes except for the minimum scaled Jacobian for the 1 hole mesh. This matches previous results that Laplacian smoothing can work well for meshes with simple boundary configurations. When compared with the Mesquite results, our method without boundary optimization produces meshes with better average scaled Jacobian in almost all cases except for the 1 hole and 3 hole 1 square. In terms of the minimum scaled Jacobian, Mesquite produces better minimum scaled Jacobian measure for five meshes, i.e., 1 hole, 3 hole, 10 holes, 3 hole 1 square, and mazewheel. It is worth noting that for patch 7, none of the existing methods can successfully untangle its inverted elements (that are highlighted by the black arrow). In contrast, our method without boundary optimization can already produce an inversion free mesh. Nevertheless, by incorporating the boundary optimization, we can produce the best quality meshes for all meshes.

Impact of the Threshold Value τ. As described earlier, a threshold value τ is used to determine when our optimization should be terminated. In our experiments, we have used different threshold values ranging from $1e^{-1}$ to $1e^{-5}$. For larger values of τ, the optimization algorithm terminates quicker as compared to smaller values of τ but the extent of optimization

Table 1: Statistics for Scaled Jacobian measure of various meshes before smoothing and after smoothing using our approach. The best quality measures are highlighted in bold. All results are obtained with the second boundary optimization approach.

			Input			Output			
Model	#V	#F	Min. Scaled Jacobian	Avg. Scaled Jacobian	Max. Scaled Jacobian	Min. Scaled Jacobian	Avg. Scaled Jacobian	Max. Scaled Jacobian	Time (s)
1 hole	69	46	0.558289	0.896226	**0.997788**	**0.742937**	**0.987127**	0.991549	0.29
2 holes	90	61	0.0146683	0.77561	0.981719	**0.701665**	**0.926261**	**0.993901**	0.526
2 holes 2 squares	140	97	-0.556381	0.735316	0.993744	**0.197108**	**0.84893**	**0.997823**	0.112
3 holes 1 square	144	96	0.553854	0.832912	0.997128	**0.724021**	**0.92366**	**0.998528**	0.111
6 holes 2 squares	352	242	-0.164996	0.750487	0.996743	**0.296134**	**0.880297**	**0.99996**	0.547
8 holes	335	229	-0.513426	0.770411	**0.999775**	**0.5811**	**0.892645**	0.999414	0.304
10 holes	288	199	-0.0984454	0.680388	0.995199	**0.411444**	**0.841136**	**0.995901**	0.407
patch 5	87	55	-0.156262	0.756085	0.998083	**0.360867**	**0.838986**	**0.999841**	0.034
patch 7	126	90	-0.528536	0.717805	**0.998884**	**0.312207**	**0.79753**	0.993506	0.06
mazewheel 3	601	392	-0.327252	0.741232	0.999852	**0.0558543**	**0.888563**	**0.999978**	0.81

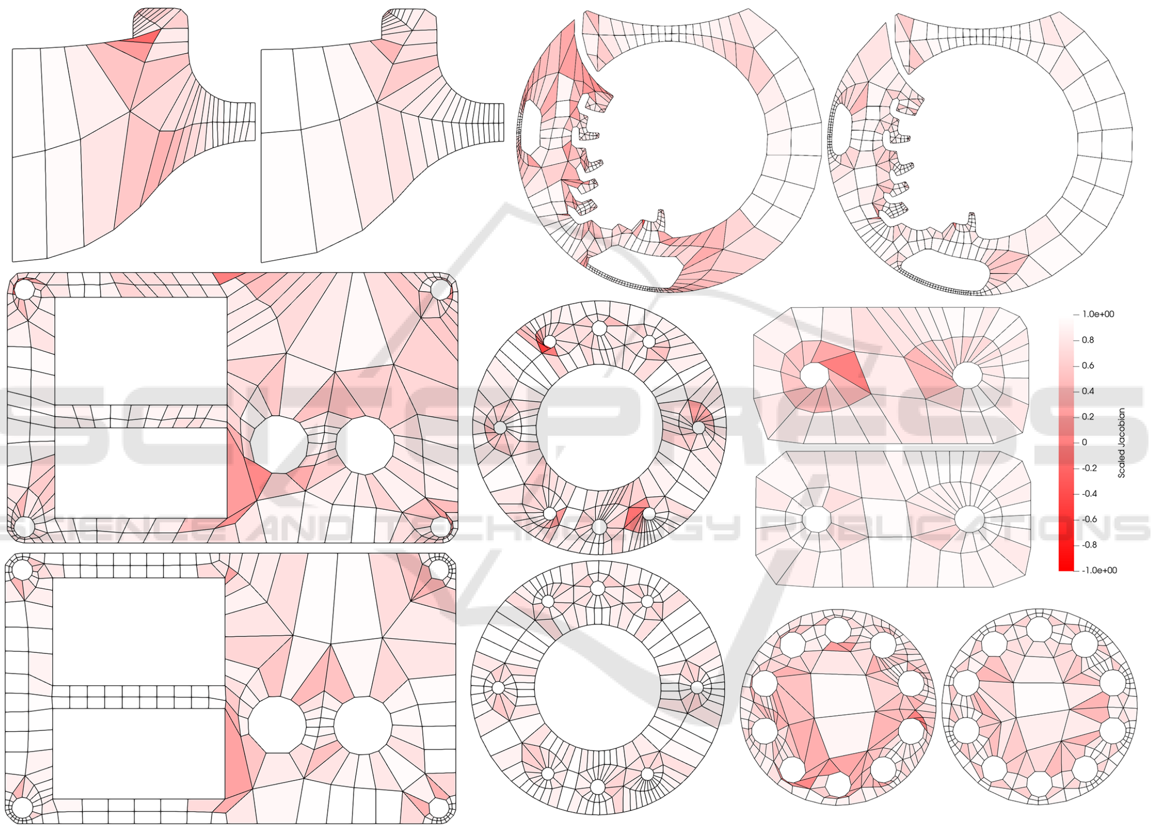

Figure 5: The representative results of the proposed method. For all meshes, the left (or top) image shows the input mesh while the right (or bottom) image is the optimized mesh with our method.

is limited. Table 3 summarizes optimization results for various meshes optimized using different values of τ. The best quality measures are highlighted in bold. As can be seen in Table 3, there is not a universally good τ value for different meshes. Thus, we leave this threshold value for the user to decide.

5 CONCLUSION

This paper presents a new quality improvement method for 2D quad meshes with open boundaries. Our method is based on the optimization of the configuration of an embedded polygon constructed for each interior vertex. A feature preserving boundary optimization is also introduced. We have applied our framework to a number of 2D quad meshes to evaluate its effectiveness. We also compare our method

Table 2: Statistics of Scaled Jacobian measures of various meshes optimized with different methods. The best quality measures of all results are highlighted in bold. The best quality measures of the results produced by methods with fixed boundaries are highlighted in blue.

	Xu and Newman		Laplacian		Mesquite		Ours w/o bound		Ours w bound	
Model	Min. Scaled	Avg. Scaled	Min. Scaled	Avg. Scaled	Min. Scaled	Avg. Scaled	Min. Scaled	Avg. Scaled	Min. Scaled	Avg. Scaled
1 hole	0.558289	0.899476	0.640883	0.899255	0.643728	0.902054	0.614279	0.8973	**0.97646**	**0.987127**
2 holes	0.166075	0.79649	-0.0158924	0.773395	0.0205342	0.774537	0.0811026	0.777924	**0.742937**	**0.926261**
2 holes 2 squares	-0.556381	0.752143	-0.453973	0.735066	-0.487485	0.738351	-0.15848	0.782632	**0.197108**	**0.84893**
3 holes 1 square	0.559189	0.842663	0.538608	0.833651	0.57367	0.838737	0.563918	0.83856	**0.724021**	**0.92366**
6 holes 2 squares	-0.164996	0.761158	-0.36941	0.749143	-0.28024	0.760459	-0.117874	0.785367	**0.296134**	**0.880297**
8 holes	-0.513426	0.767459	-0.544005	0.765766	-0.47977	0.772616	-0.147611	0.788872	**0.5811**	**0.892645**
10 holes	-0.0984454	0.783175	-0.246311	0.675738	-0.188317	0.686278	-0.201791	0.708256	**0.411444**	**0.841136**
patch 5	-0.0247695	0.776693	-0.176222	0.750139	-0.15496	0.759693	-0.0813105	0.818403	**0.360867**	**0.838986**
patch 7	-0.528536	0.724826	-0.147158	0.727404	-0.556283	0.728614	0.276863	0.789242	**0.312207**	**0.79753**
mazewheel 3	-0.458242	0.745167	-0.699953	0.735654	-0.653876	0.742469	-0.65144	0.761198	**0.0558543**	**0.888563**

Table 3: Effect of different threshold (τ) values on mesh optimization using our method on a number of representative meshes. The best quality measures are highlighted in bold.

	$\tau = 0.1$		$\tau = 0.01$		$\tau = 0.001$		$\tau = 0.0001$		$\tau = 0.00001$	
Model	Min. Scaled	Avg. Scaled	Min. Scaled	Avg. Scaled	Min. Scaled	Avg. Scaled	Min. Scaled	Avg. Scaled	Min. Scaled	Avg. Scaled
2 holes 2 squares	0.197108	0.847687	0.197108	**0.849726**	0.197108	0.849073	0.197108	0.84893	0.197108	0.84893
3 holes 1 square	0.720105	0.920828	0.721011	**0.923883**	0.723246	0.923717	0.724021	0.92366	**0.724161**	0.923631
6 holes 2 squares	0.318459	**0.882613**	**0.320006**	0.880864	0.298935	0.880412	0.296134	0.880297	0.29614	0.880295
8 holes	**0.58685**	0.891942	0.582073	**0.892883**	0.580989	0.89271	0.5811	0.892645	0.581242	0.892652
10 holes	0.413944	**0.843625**	0.411547	0.841411	0.411444	0.841136	0.411444	0.841136	**0.449502**	0.841136
patch 7	0.251875	0.794919	0.303568	0.797214	0.303568	0.797214	**0.312207**	**0.79753**	**0.312207**	**0.79753**
mazewheel 3	0.0066067	**0.88877**	0.0411956	0.88851	0.0518666	0.888541	0.0558543	0.888563	**0.0566735**	0.888568

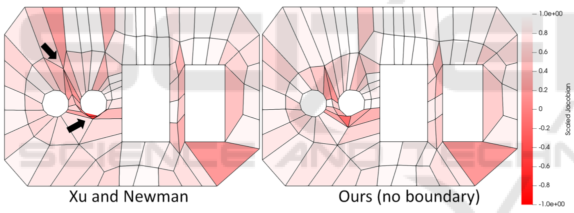

Figure 6: Comparison of our method (right) with Xu and Newman's approach (left). The arrows indicate places that the mesh quality in the results of Xu and Newman's approach is less desired. The 2 holes with 2 square mesh is shown. Red color indicate quad elements with low Jacobian measures.

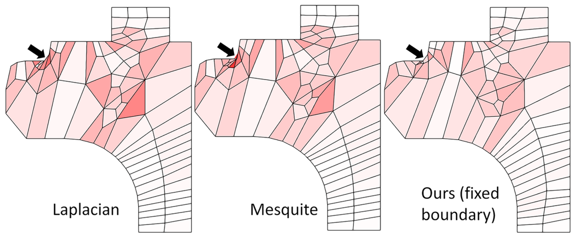

Figure 7: Comparison with conventional Laplacian smoothing with cotangent weights and the Laplacian smoothing implemented in Mesquite. The patch 7 mesh is shown. Red color indicate quad elements with low Jacobian measures. The arrows highlight area with elements that other methods fail to improve, while our method can.

with a number of the state-of-the-art quad mesh optimization methods. The comparison shows that our method outperforms the existing methods in most cases, especially for meshes with many complicated boundary features.

Limitation and Future Work. Even though our method is simple and easy to implement and has shown outperforming many state-of-the-art methods in most cases, our method cannot guarantee to always produce inversion-free mesh. As shown in the inset, our method fails to untangle an inverted element in the mazewheel mesh. A closer look shows that three vertices of this inverted element are on the boundary, and two of them are corners, thus, fixed. These three vertices form a concave configuration with an inner angle larger than 180°.

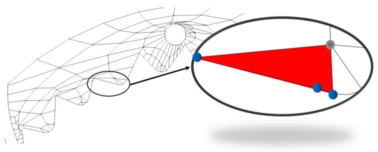

In fact, no smoothing method can fix this unless this boundary is modified to make the angle smaller than 180°. Alternatively, a local connectivity modification may help mitigate this situation, which is beyond the scope of this work.

Our current framework provides two different ways for boundary optimization. In the future, it will be more ideal to have an automatic way to decide the proper boundary optimization based on the input mesh configuration without user intervention.

ACKNOWLEDGEMENTS

We thank the anonymous reviewers for their valuable feedback. This research was partially supported by NSF IIS 1553329.

REFERENCES

Ben-Chen, M., Gotsman, C., and Bunin, G. (2008). Conformal flattening by curvature prescription and metric scaling. In *Computer Graphics Forum*, volume 27, pages 449–458. Wiley Online Library.

Bommes, D., Lévy, B., Pietroni, N., Puppo, E., Silva, C., Tarini, M., and Zorin, D. (2013). Quad-mesh generation and processing: A survey. In *Computer Graphics Forum*, volume 32, pages 51–76. Wiley Online Library.

Bommes, D., Zimmer, H., and Kobbelt, L. (2009). Mixed-integer quadrangulation. *ACM Trans. Graph.*, 28(3).

Brewer, M. L., Diachin, L. F., Knupp, P. M., Leurent, T., and Melander, D. J. (2003). The Mesquite Mesh Quality Improvement Toolkit. In Shepherd, J., editor, *IMR*.

Campen, M. (2017). Partitioning surfaces into quadrilateral patches: a survey. In *Computer Graphics Forum*, volume 36, pages 567–588. Wiley Online Library.

Canann, S. A., Tristano, J. R., Staten, M. L., et al. (1998). An approach to combined laplacian and optimization-based smoothing for triangular, quadrilateral, and quad-dominant meshes. In *IMR*, pages 479–494. Citeseer.

Daniels, J., Silva, C. T., and Cohen, E. (2009). Localized quadrilateral coarsening. In *Computer Graphics Forum*, volume 28, pages 1437–1444. Wiley Online Library.

Docampo-Sanchez, J. and Haimes, R. (2019). Towards fully regular quad mesh generation. In *AIAA Scitech 2019 Forum*, page 1988.

Fang, X., Bao, H., Tong, Y., Desbrun, M., and Huang, J. (2018). Quadrangulation through morse-parameterization hybridization. *ACM Transactions on Graphics (TOG)*, 37(4):92.

Gao, X., Deng, Z., and Chen, G. (2015). Hexahedral mesh re-parameterization from aligned base-complex. *ACM Transactions on Graphics (TOG)*, 34(4):1–10.

Gao, X., Huang, J., Xu, K., Pan, Z., Deng, Z., and Chen, G. (2017). Evaluating hex-mesh quality metrics via correlation analysis. In *Computer Graphics Forum*, volume 36, pages 105–116. Wiley Online Library.

Ji, Z., Liu, L., and Wang, G. (2005). A global laplacian smoothing approach with feature preservation. In *Ninth International Conference on Computer Aided Design and Computer Graphics (CAD-CG'05)*, pages 6–pp. IEEE.

Kim, J., Choi, J., and Kang, W. (2020). A data-driven approach for simultaneous mesh untangling and smoothing using pointer networks. *IEEE Access*, 8:70329–70342.

Kim, J., Shin, M., and Kang, W. (2015). A derivative-free mesh optimization algorithm for mesh quality improvement and untangling. *Mathematical Problems in Engineering*, 2015.

Pébay, P. P., Thompson, D. C., Shepherd, J., Knupp, P. M., Lisle, C., Magnotta, V., and Grosland, N. M. (2007). New Applications of the Verdict Library for Standardized Mesh Verification Pre, Post, and End-to-End Processing. In Brewer, M. L. and Marcum, D. L., editors, *IMR*, pages 535–552. Springer.

Pietroni, N., Tarini, M., and Cignoni, P. (2009). Almost isometric mesh parameterization through abstract domains. *IEEE Transactions on Visualization and Computer Graphics*, 16(4):621–635.

Prasad, T. (2018). *A comparative study of mesh smoothing methods with flipping in 2D and 3D*. PhD thesis, Rutgers University-Camden Graduate School.

Sorkine, O. (2005). Laplacian Mesh Processing. In Chrysanthou, Y. and Magnor, M., editors, *Eurographics 2005 - State of the Art Reports*. The Eurographics Association.

Tarini, M., Pietroni, N., Cignoni, P., Panozzo, D., and Puppo, E. (2010). Practical quad mesh simplification. In *Computer Graphics Forum*, volume 29, pages 407–418. Wiley Online Library.

Tarini, M., Puppo, E., Panozzo, D., Pietroni, N., and Cignoni, P. (2011). Simple quad domains for field aligned mesh parametrization. In *Proceedings of the 2011 SIGGRAPH Asia Conference*, pages 1–12.

Vartziotis, D. and Himpel, B. (2014). Laplacian smoothing revisited. *arXiv preprint arXiv:1406.4333*.

Viertel, R. and Osting, B. (2019). An approach to quad meshing based on harmonic cross-valued maps and the ginzburg–landau theory. *SIAM Journal on Scientific Computing*, 41(1):A452–A479.

Xu, H. and Newman, T. S. (2005). 2d fe quad mesh smoothing via angle-based optimization. In *International Conference on Computational Science*, pages 9–16. Springer.

Xu, K., Gao, X., and Chen, G. (2018). Hexahedral mesh quality improvement via edge-angle optimization. *Computers & Graphics*, 70:17–27.

Zhang, Y., Bajaj, C. L., and Xu, G. (2005). Surface Smoothing and Quality Improvement of Quadrilateral/Hexahedral Meshes with Geometric Flow. In Hanks, B. W., editor, *IMR*, pages 449–468. Springer.

Zhou, T. and Shimada, K. (2000). An angle-based approach to two-dimensional mesh smoothing. *IMR*, 2000:373–384.